4-1-2019

Analysis of operational parameters, reactor kinetics, and floc characterization for the removal of estrogens via electrocoagulation

Emily K. Maher
Marquette University

Kassidy N. O'Malley
Marquette University

Joe Heffron
Marquette University

Jingwan Huo
Univesity of Wisconsin - Milwaukee

Brooke K. Mayer
Marquette University, Brooke.Mayer@marquette.edu

See next page for additional authors

Accepted version. *Chemosphere*, Vol. 220 (April 2019): 1141-1149. DOI.

Analysis of operational parameters, reactor kinetics, and floc characterization for the removal of estrogens via electrocoagulation

Emily K. Maher
Department of Civil, Construction and Environmental Engineering, Marquette University, Milwaukee, WI
Kassidy N. O'Malley
Department of Civil, Construction and Environmental Engineering, Marquette University, Milwaukee, WI
Joe Heffron
Department of Civil, Construction and Environmental Engineering, Marquette University, Milwaukee, WI
Jingwan Huo
Department of Civil and Environmental Engineering, University of Wisconsin-Milwaukee, Milwaukee, WI
Brooke K. Mayer
Department of Civil, Construction and Environmental Engineering, Marquette University, Milwaukee, WI

Yin Wang
Department of Civil and Environmental Engineering, University of Wisconsin-Milwaukee, Milwaukee, WI
Patrick J. McNamara
Department of Civil, Construction and Environmental Engineering, Marquette University, Milwaukee, WI

Abstract

Estrogenic compounds can cause human and ecological health issues and have been detected in surface and drinking water. In this research a reactor analysis determined the impact of operational parameters, the best fit kinetic model for the removal of estrone (E1), 17β-estradiol (E2), estriol (E3), and 17α-ethynylestradiol (EE2) using a bench-top iron electrocoagulation reactor, and characterized the floc generated *in-situ*. The parameters investigated were current density, conductivity, stir rate, and polarity reversal. Estrogen removal correlated well with an increase in current density, while conductivity did not impact removal but did reduce potentials. High stir rates and frequent polarity reversal demonstrated greater removal. The operating parameters that achieved the greatest estrogen removal were a current density of 16.7 mA cm^{-2}, conductivity of 1000 μS cm^{-1}, stir rate of 500 rpm, and a polarity reversal time of 30 s. These parameters led to average removal efficiencies of 81%, 87%, 85%, and 97% for E1, E2, E3, and EE2, respectively. The removal data for all estrogenic compounds best fit a pseudo-first order relationship with kinetic rate constants of 0.015 min^{-1} for E1 and E2, 0.016 min^{-1} for E3 and 0.040 min^{-1} for EE2. The floc formed *in-situ* were characterized by determining the crystalline phases with X-ray diffraction, the size and zeta potential, and the shape and major components using scanning electron microscope with energy-dispersive X-ray spectrometer. The iron coagulant generated during electrocoagulation was lepidocrocite with a point of zero charge of 5.67 and an average floc diameter of 2255 nm.

Keywords

Estrone (E1), 17β-estradiol (E2), Estriol (E3), 17α-ethynylestradiol (EE2), Drinking water, Iron,Floc

1. Introduction

Estrogenic compounds are endocrine disrupting compounds (EDCs) that can mimic, increase, or inhibit endogenous hormones, consequently altering the natural function of the endocrine system in humans and animals (Roy et al., 2009; Silva et al., 2012). Observed impacts include feminization of fish populations in both wild and controlled studies (Kidd et al., 2007; Vajda et al., 2008). Human health impacts include male and female reproductive health issues, precocious puberty, cancer, and increased rates of obesity and diabetes (Roy et al., 2009; National Institute of Environmental Health Sciences, 2010).

Estrogenic compounds in wastewater, surface water, and drinking water have received increased attention in recent years due to their potential to negatively impact human and environmental health, including increased research on treatment technologies to remove estrogens (Kolpin et al., 2002; Snyder et al., 2003; Westerhoff et al., 2005; Kidd et al., 2007; Vajda et al., 2008; Benotti et al., 2009b; Caldwell et al., 2010). Estrogens make their way into drinking water as a result of incomplete

removal during wastewater treatment, subsequent discharge to surface water, and eventual intake during drinking water treatment (Ternes, 1998; Daughton and Ternes, 1999; Kuch and Ballschmiter, 2001; Kolpin et al., 2002; Snyder et al., 2003; Westerhoff et al., 2005; Benotti et al., 2009a; Caldwell et al., 2010; Conley et al., 2017). Consequently, populations served by municipal drinking water treatment facilities are at risk of exposure to these estrogens.

As a result of the potential risks and presence of estrogens in environmental waters, the United States Environmental Protection Agency's (USEPA) Contaminant Candidate List version 4 (CCL4) includes estrone (E1), 17β-estradiol (E2), estriol (E3), and 17α-ethynylestradiol (EE2). The USEPA CCL4 is comprised of emerging contaminants not regulated by drinking water standards, but which are likely present in public drinking water systems and are of interest due to potential public health risks. Compounds listed on the CCL require more research to understand their potential for removal by conventional and advanced treatment processes before regulatory determinations (US EPA, 2016).

Removal of estrogenic compounds within drinking water treatment is limited and variable; conventional coagulation/flocculation treatment processes used for the treatment of surface water were not designed to remove estrogenic compounds. Westerhoff et al. (2005) evaluated a simulated coagulation/flocculation process that used alum and ferric chloride as coagulants and demonstrated that removals of E1, E2, and EE2 were 5%, 2%, and 0%, respectively (Westerhoff et al., 2005). This result was unexpected due to the low volatility and hydrophobic nature of E1, E2, E3, and EE2 (i.e. Log K_{OW}, Tables S1 and SI section S1), indicating they would be likely candidates to sorb to solids (i.e. iron oxides) (Lai et al., 2000; Silva et al., 2012). In response to their minimal removal, alternatives to conventional water treatment have been investigated for the removal of estrogenic compounds as part of point-of-use, emergency, and municipal treatment systems.

Advanced oxidation processes (AOPs), including ozone (O_3), ozone and hydrogen peroxide (O_3/H_2O_2), and electrooxidation (EO), have offered exceptional removal of estrogens (Snyder et al., 2004, 2006; Westerhoff et al., 2005; Benotti et al., 2009a; Liu et al., 2009; Feng et al., 2010a; Chen and Huang, 2013; Cong et al., 2014). Electrocoagulation (EC) is an additional technology that may provide greater estrogen removal than conventional coagulation/flocculation systems alone because EC provides *in-situ* coagulant generation together with redox potential (Mollah et al., 2004; Heidmann and Calmano, 2008; Liu et al., 2010). EC uses sacrificial electrodes, typically iron or aluminum, to produce metal hydroxide flocs *in-situ* (Mollah et al., 2004; Liu et al., 2010). EC flocs are crystalline in structure, fractal and highly porous with large surface areas (Cornell et al., 2003; Lin et al., 2015). Estrogenic compounds may also be removed via redox reactions at the anode or cathode as well as indirect redox reactions in solution. These reactions may derive from interactions with hydroxyl radical ($OH^{\cdot}$) generation or the formation of high valence iron species, such as ferryl iron (Fe(IV)), through intermediate iron reactions (Mollah et al., 2004; Heidmann and Calmano, 2008; Keenan and Sedlak, 2008; Liu et al., 2010; Li et al., 2012).

EC is capable of removing a variety of water pollutants, including turbidity, chemical oxygen demand, biochemical oxygen demand, phosphate, and color in wastewaters (Rajeshwar et al., 1994; Pan et al., 2016). In drinking water treatments, EC has been shown to remove heavy metals (Heidmann and Calmano, 2008; Heffron et al., 2016), polyfluoroalkyl acids (PFAAs) (Lin et al., 2015), and some pharmaceuticals (e.g. sulfamethoxazole and trimethoprim) (Mission et al., 2010; Martins et al., 2011; Ghatak, 2014). EC may be most useful in small-scale, rural, drinking water treatment

systems or as a pretreatment technology for electrooxidation to remove organics upfront. EC has the potential to remove estrogens from drinking water, which are typically removed <5% using conventional coagulation and flocculation (Westerhoff et al., 2005; Yoshihara and Murugananthan, 2009). In addition, compared to conventional coagulation and flocculation technologies, EC has a smaller footprint, and lower chemical requirements than conventional coagulation/flocculation systems (Mollah et al., 2004). Accordingly, previous studies have demonstrated that EC is capable of removing organic constituents (Mission et al., 2010; Martins et al., 2011; Ghatak, 2014; Lin et al., 2015); however, no known research has determined the effectiveness of EC for removal of estrogenic compounds. EC may be beneficial as a pretreatment technology due to its ability to create a number of removal mechanisms in addition to its small footprint and low chemical requirements (Mollah et al., 2004; Heidmann and Calmano, 2008; Keenan and Sedlak, 2008; Liu et al., 2010; Li et al., 2012).

While iron-based EC offers potential to remove estrogenic compounds, no known research has been conducted to characterize its effectiveness and the role of reactor operational parameters. Several parameters are important for the operation of an EC reactor, including current density, conductivity, stir rate, and polarity reversal (Chen et al., 2000; Liu et al., 2010; Dubrawski and Mohseni, 2013). Current density (i, mA cm^{-1}) is the current per unit area of active anode surface and is very important as it is the easiest operational parameter to control within the laboratory (Liu et al., 2010). The current density influences the coagulant dose to the EC system and will directly influence the removal of estrogens. If the conductivity is low, it will reduce current efficiency, increase required applied potential, and consequently increase passivation and also treatment cost (Liu et al., 2010). Increased turbulence within the reactor can present a number of potential advantages and disadvantages. For example, it may increase metal ion mass transport into solution (Mollah et al., 2004), but may also break up floc, and thus decrease removal (Crittenden et al., 2012a, b). Finally, polarity reversal is the intermittent alternation of the polarity between the two electrodes (Mollah et al., 2004). Polarity reversal has shown to reduce the detrimental impacts of the electrode passivation, which is the formation of an inhibiting oxide layer on the surface of the electrode over time (Liu et al., 2010). As the thickness of the passivation layer increases, the efficiency of the EC reactor decreases due to reduced metal dissolution, electron transfer, and overall coagulant dose (Liu et al., 2010). Investigating the influence of these parameters for an EC system is important to better understand the efficiency and effectiveness of EC as a technology to remove organic micro-contaminants.

The primary objective of this study was to determine how reactor operation parameters impact removal of estrogens using iron EC. The impact of current density, conductivity, stir rate, and polarity reversal time on the removal of estrogenic compounds was determined. A reactor analysis was also conducted in which the removal kinetics were assessed and the generated iron oxide floc was characterized. To our knowledge, this is the first study to examine the impact of stir rate and polarity reversal, as well as establish the degradation kinetics of E1, E2, E3, and EE2 in an iron EC process.

2. Materials and methods

2.1. Chemicals

Stock solutions of E1, E2, E3, and EE2 were prepared in HPLC-grade methanol (≥99%) purchased from Alfa Aesar (West Hill, MA) and were stored at −20 °C. E1 (≥99% purity), E2 (≥98%), E3 (≥97%), EE2 (≥98%), sodium sulfate (≥99%), and sodium nitrate (≥99%) were purchased from Sigma-Aldrich (St.

Louis, MO). Sulfuric acid (96.6%) and sodium bicarbonate were purchased from Fisher Scientific International, Inc. (Fair Lawn, NJ).

2.2. Electrocoagulation cell construction

The EC reactors were 500 mL Berzelius beakers with no pour spout with a 3D printed plastic cap designed to accommodate two sacrificial electrodes with a fixed electrode distance of 1 cm. The electrodes were iron (mild steel) plates with an active anode surface area of 60 cm^2. In all cases, a direct current was supplied by a benchtop DC regulated power source (Sorensen XPH75-2D, 300 W, 0–75 W, 0–2 A, dual output, universal input 110VAC to 240VAC) paired with a current alternator (kindly provided by A/O Smith Corporation, Brookfield, WI). Polarity reversal impact on estrogen removal was investigated at frequencies of 30, 120, and 240 s. Completely mixed batch reactors were agitated with a multi-position magnetic stirrer. Each test was conducted for 120 min until equilibrium was reached.

All glassware, stir bars, and caps were washed with Alconox®, rinsed, dried and triple rinsed in methanol. Sample vials (4 mL glass amber) were baked at 550 °C for 45 min and cooled to remove any residual organics. Preliminary control tests indicated negligible adsorption of the estrogens to the glassware. Between experiments, the electrodes were cleaned similar to Dubrawski and Mohseni (2013) (Dubrawski and Mohseni, 2013). Briefly, the electrodes were cleaned using an acid wash in 2 M sulfuric acid, rinsed with water, washed with an abrasive scrubber with Alconox®, wet sanded with 320 grit fine sand paper, and sonicated in methanol for 20 min.

2.3. Experiments

Current density (*i*), conductivity, stir rate, and polarity reversal time were selected and tested individually in a batch EC reactor with two iron plate electrodes to determine the best operating parameters for this system for consequent experiments. All tests were conducted in at least triplicate at room temperature.

Current density can be directly controlled with either electrode area or current (Holt et al., 2005; Dubrawski and Mohseni, 2013). The current density is directly related to the iron oxide dosing rate, mass transfer, and redox reactions occurring at the electrode surface (Holt et al., 2005). Faraday's law (Eq. (1)) describes the relationship between current density (*j*; mA cm^{-2}) and the mass of metal dissolved (*w*; g cm^{-2}) using the time of electrolysis (*t*; s), the molar mass of the electrode material (*M*; g mol^{-1}), the number of electrons transferred in anodic dissolution (*n*), and Faraday's constant (*F*, C mol^{-1}).

$$(1) W = \frac{jtM}{nF}.$$

Three current densities (4.16, 8.3, and 16.7 mA cm^{-2}) were examined at various conductivity values (500, 1000, and 3000 µS cm^{-1}) to determine the combination that achieved greatest estrogenic compound removal. Using the current density and conductivity that achieved the greatest removal of estrogenic compounds in initial tests, the impact of three stir rates (50, 120, and 500 rpm) and three polarity reversal times (30, 120, 240 s) were examined in triplicate experiments.

For each experiment, a synthetic test water was prepared in Milli-Q (Millipore) water with a conductance of 18.2 MΩ at 25 ± 1 °C. Electrolyte concentrations were added to achieve a concentration of 2.25 mM (500 µS cm^{-1}), 4.51 mM (1000 µS cm^{-1}), or 13.52 mM (3000 µS cm^{-1}) with sodium sulfate. Alkalinity was added with sodium bicarbonate to a concentration of 85 mg L^{-1} as

$CaCO_3$. The pH was adjusted to 7.0 with either sodium hydroxide or sulfuric acid. Estrogen stock solutions were added to the bulk solution to obtain a concentration of approximately 200 µg L^{-1}. The methanol cosolvent effects were negligible as the volumetric fraction of methanol to water was 0.2% (Tong et al., 2016).

Samples (1 mL) were collected at varying times depending upon the test type, mixed with 1 mL methanol and filtered through 0.2 µm, 13 mm, PTFE Agela Technologies (Wilmington, DE) syringe filter (to eliminated retaining estrogens on the filter) into a glass amber 1.5 mL LC-MS vial. Sample collection did not impact current density by greater than 5%. Spike and recovery tests were conducted for the estrogens. Recovery of estrogens (average ± standard deviation) was 92 ± 1.1% for E1, 104 ± 2.4% for E2, 86 ± 1.6% for E3, and 100 ± 1.8% for EE2 (n = 3) using PTFE filters.

2.4. Analytical measurements

Estrogens (~200 µg L^{-1}) were analyzed by liquid chromatography mass spectrometry (LC-MS) using a Shimadzu LC-MS 2020 equipped with a Phenomenex® Kinetex® 5 µ EVO C18 100 A 100 × 3.0 mm reversed phase column operated in negative ion mode for all compounds (see Section S2 in the SI for LCMS operation conditions). Section S3 in the SI outlines the criteria for the standard curve, limit of detection (LOD), and limit of quantification (LOQ). The pH was measured before and after each test using an Orion 4 Star pH meter (Thermo Scientific, USA) and the conductivity was measured using a VWR® Pure H_2O Tester (VWR, Radnor, PA); test data are provided in Section S4, Table S4. Iron doses were measured as total iron via inductively coupled plasma mass spectrometry after acid digestion (ICP-MS) analysis (7700 Series, Agilent Technologies, Santa Clara, CA, USA).

2.5. Kinetics analysis

Pseudo-first order, second-order, Lagergren's pseudo first-order, and Lagergren's second-order equation for adsorption kinetics were evaluated to describe the removal reaction kinetics for this study (Khatibikamal et al., 2010; Al-Shannag et al., 2015; Moussout et al., 2018). For the EC batch process, the law of mass of conservation was considered (Eq. (3)):

$$(3)\quad -\frac{dC}{dt} = -r_D$$

Where $-r_D$ is the removal rate of estrogens, C is the concentration (µg/L) and t is the EC time in min. The pseudo first-order model and integration are described in Eq. (4) and Eq. (5), where C (0) = C_0. The pseudo first-order model rate takes into account a potential catalyst with a concentration is negligible where r = k(C)(A) = k'(C). Where the solution is given by Eq. (5) (Al-Shannag et al., 2015).

$$(4)\quad C = C_o e^{-k't}$$

$$(5)\quad \ln\left(\frac{C}{C_o}\right) = -k't$$

where k' is the pseudo first-order rate constant in min^{-1}.

The second-order rate model follows $-r = k_2C^2$, where k_2 is the second order rate constant. The equation solution is defined in Eq. (6).

$$(6)\frac{1}{C} = \frac{1}{C_o} + k_2 t$$

The kinetic data was also analyzed using Lagergren's pseudo first- and second-order rate equations (Khatibikamal et al., 2010). These data were calculated using the assumption that all estrogen removal was due to adsorption to the iron oxide floc. Lagergren's pseudo first-order model is (Eq. (7)):

$$(7) -\frac{dq}{dt} = k_1(q_e - q)$$

Where q is the amount of estrogenic compounds adsorbed to the adsorbent (iron floc) at a time t (min), q_e is the amount of estrogenic compounds present at equilibrium and k_1 (min^{-1}) is the first-order adsorption rate constant. The integrated linear form of the equation is defined in Eq. (8), where the q_e and k_1 were calculated from the slope and y-intercept of the plots.

$$(8)\log(q_e - q) = \log(q_e) - \frac{k_t t}{2.303}$$

The pseudo-second order rate is expressed in Eq. (9) and the integrated form is in Eq. (10).

$$(9) -\frac{dq}{dt} = k_2(q_e - q)^2$$

$$(10)\frac{t}{q} = \frac{1}{k_2 q_e^2} + \frac{t}{q_e}$$

where k_2 is the second order rate constant. The q_e and k_2 were calculated from the slope and intercept of the plot of t/q versus time (t).

2.6. Floc characterization

Floc characterization was conducted to understand and investigate the structure, and general behavior of the iron hydroxide floc within iron EC. After EC, the metal hydroxide flocs were freeze dried using a Millrock Technology bench top freeze dryer (Kingston, NY). Zeta potential and average size of the iron hydroxide flocs were measured with a Malvern Zetasizer Nano ZS (Malvern Instruments, UK). The point of zero charge was determined by using the zeta potential provided by the instrument, completing a linear regression, using the line equation to calculate it via interpolation as the pH where zeta potential was zero. X-ray diffraction (XRD) of the iron floc was carried out with a Bruker D8 Discover A25 diffractometer with a copper Kα radiation to determine the crystalline structure of the various flocs formed. The XRD scans were recorded from 2ϑ of 10°–70° using a step size of 0.02° and a count time of 0.4 s per step. Scanning electron microscope (SEM) with an energy-dispersive X-ray spectrometer (EDX) (JEOL; JEOL USA, Inc. MA, USA; JSM-6510LV SEM) was used to investigate the morphology and composition of the floc as well as the major elemental components. The sample was coated with a conductive gold/palladium spray and adhered to an SEM mount with double-sided carbon tape.

2.7. Statistical analysis

Statistical data analysis was performed using Graphpad Prism 7® (Graphpad Software, La Jolla, CA). A one-way analysis of variance (ANOVA) was performed for each compound for each parameter tested.

Data sets with values greater than zero percent removal underwent a logit transformation. Data sets containing zero percent removal underwent an arcsine transformation. Post-hoc tests were performed with the Tukey's multiple comparisons test. All error bars on figures represent the standard error of the mean. Correlation analyses were conducted using linear correlation measured by the Pearson's correlation coefficient (Pearson's r).

3. Results and discussion

3.1. Parameters

3.1.1. Impact of current density and conductivity

Current density had substantial impact on estrogenic removal (Fig. 1). The current density was altered by changing the current while maintaining the submerged electrode surface area, EC time, conductivity, polarity reversal time, and stir rate. Increasing the current increased estrogenic compound removal (Fig. 1) and the charge loading rate (CLR) (C L^{-1} min^{-1}) (Dubrawski and Mohseni, 2013). The greatest removal for all compounds was achieved with a current density of 16.7 mA cm^{-2}. The results in Fig. 1 agree with other studies conducted on organic micropollutants in which increasing current density (due to increasing current) led to increased removal efficiency (Dubrawski and Mohseni, 2013). The CLR is tantamount to the dosing rate (mg L^{-1} min^{-1}), which is the rate of coagulant production normalized to the reactor volume (Dubrawski and Mohseni, 2013). Therefore, increasing the current increases the dose of the *in-situ* generated coagulant and the number of redox reactions occurring at the anode, as there is an increase in electron transfer at the electrode surface (Mollah et al., 2004). The CLRs and theoretical dosing rates associated with each current density tested were: 60C L^{-1} min^{-1}, 8.7 mg L^{-1} min^{-1} for 4.16 mA cm^{-2}; 120C L^{-1} min^{-1}, 17.4 mg L^{-1} min^{-1} for 8.3 mA cm^{-2}; and 240C L^{-1} min^{-1}, 34.7 mg L^{-1} min^{-1}, for 16.7 mA cm^{-2}. In this study, the potential increased from 8.57 to 14.5 V when the current density increased from 8.3 to 16.7 mA cm^{-2}, at a constant conductivity of 1000 µS cm^{-1}. There was a strong correlation between current density and percent removal for E1, E2, and E3 with Pearson r-values of 0.95, 0.96, and 0.93, respectively.

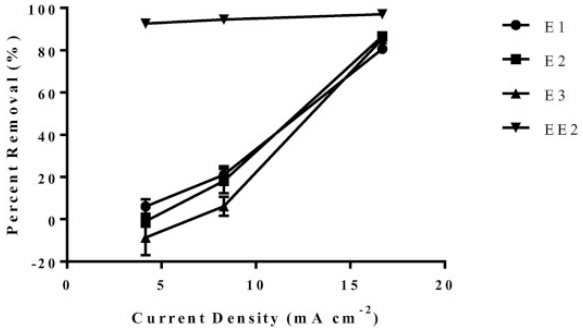

Fig. 1. The impact of current density on estrogen removal. The error bars represent the standard error of the mean.

Conductivity did not largely influence estrogen removal (see Section S5, Fig. S1, in the SI). There was no statistical difference in removal of E1, E2, and E3 between 1000 and 3000 µS cm^{-1} (p-value ≥ 0.05). However, removal of E1, E2, and E3 was significantly different between 500 and 1000 µS cm^{-1} and between 500 and 3000 µS cm^{-1} (p-values ≤ 0.002). There was no statistical difference between removals of EE2 for all conductivities (p-value = 0.7862). A well designed EC reactor for drinking water treatment should have the lowest possible IR-drop (overpotential due to solution resistance) to increase reactor efficiency (Mollah et al., 2004). The resistance is impacted by solution conductivity, electrode surface area, and electrode distance (Mollah et al., 2004). Thus, increasing the conductivity decreased the IR-drop and increased the estrogen removal (Mollah et al., 2004). The increase in

conductivity decreased applied potential; however, there was not as significant of correlation between percent removal and conductivity for E3 (Pearson r = 0.445) and EE2 (Pearson r = −0.2709) or for E1 (Pearson r = 0.504) and E2 (Pearson r = 0.5317) as there was for current density.

3.1.2. Impact of stir rate

Three stir rates were investigated in this study: 50, 120, 500 rpm. The greatest removal was achieved with a stir rate of 500 rpm (Fig. 2). The mean removals were significantly different among the compounds (ANOVA, p-value < 0.0001) and in all post-hoc analyses (Tukey, p-values < 0.0095). Therefore, as described in Mollah et al. (2004), the increased velocity over the electrode surface enhanced mass transport, direct and indirect oxidation of organics, and may have also decreased the passivation layer on the surface of the electrode, all of which improved overall removal of estrogens (Mollah et al., 2004). Increasing the turbulence (velocity over the electrodes) within the reactor likely increased the mass transfer of the metal ions from the anode surface into the bulk solution, thus reducing flux into solution (Mollah et al., 2004). The increased removal indicated that higher stir rates favor oxidation reactions over adsorption for the removal of estrogens. Typically, higher stir rates increase the potential to break up floc due to shear forces, as is typical in conventional coagulation and flocculation processes and decrease removal of contaminants (Crittenden et al., 2012a, b). Future work should consider examining the particle size of the floc at each stir rate to confirm the possible change in floc size. Additionally, high stir rates can decrease the hydrodynamic boundary layer and increase the rate of diffusion to an electrode surface for solutions with very low reactant concentration and thus increase the oxidation and removal of estrogens within the solution (Bagotsky, 2005). Overall, the higher stir rates increase velocity and thus increase the electron transfer flux between the electrode surface and the bulk solution and as a result increase estrogen removal.

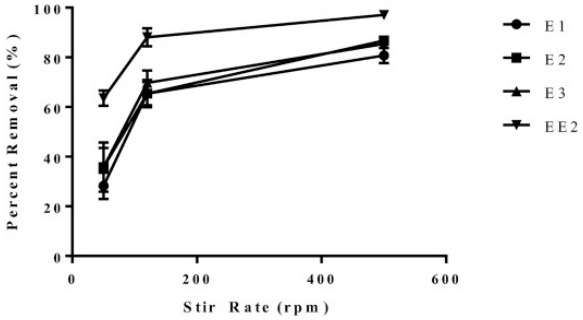

Fig. 2. The impact of stir rate on estrogen removal. The error bars represent the standard error of the mean.

3.1.3. Impact of polarity reversal

The shortest polarity reversal time tested, 30 s, yielded the highest removal for E1, E2, and E3 (Fig. 3, ANOVA, p-values ≤ 0.0032; Tukey, p-values ≤ 0.35). There was no significant difference between 120 and 240 s for E1, E2, or E3 (Tukey, p-values ≥ 0.093). The percent removals were calculated based on the LOD for these specific tests because EE2 was below detection. The shorter polarity reversal increased overall removal by inhibiting the formation of the passivation layer. Electrode passivation, the formation of an insulating oxide layer on the electrode surface, is detrimental to reactor performance and can be mitigated by periodic reversal of electrode polarity to improve reactor performance (Mollah et al., 2004; Liu et al., 2010). Passivation thickness increases with time and inhibits electron transfer between the electrode and contaminant (Liu et al., 2010). Thus, the change in polarity is capable of reducing the negative impacts of the passivation layer on estrogen removal by increasing the potential and decreasing the barrier to electron transfer (Mollah et al., 2004). The

concentration of the estrogens in solution will equal the concentration at the surface of the electrode after switching the polarity because the estrogens are not charged. The concentration will gradually approach zero if the current is high enough to overtake the rate of diffusion to the electrode surface and then decrease the estrogen concentration in the bulk solution. The polarity reversal may be seen as concentration gradient control. It is common to reverse polarity during bench scale testing (Timmes et al., 2010; Mohora et al., 2012), however, reporting on the impact on the reversal time in iron EC bench scale reactors for the removal of organic contaminants in previous reports is limited.

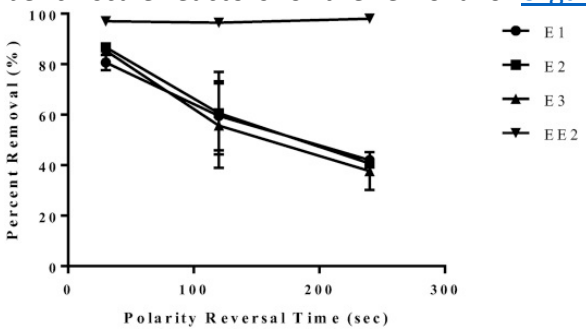

Fig. 3. The impact of polarity reversal time on estrogen removal. The error bars represent the standard error of the mean.

3.1.4. Potential removal mechanisms

The potential removal mechanisms during EC include adsorption to the iron floc, oxidation via intermediate reactions occurring in solution, and direct anodic oxidation (Mollah et al., 2004; Heidmann and Calmano, 2008; Liu et al., 2010). The increase in current improved estrogen removal, likely by increasing the mass of metal ions transported from the anode surface to the bulk solution (Mollah et al., 2004). Additionally, the increase in current would increase redox reactions occurring within the solution and at the electrode surface thus increasing estrogen degradation (Mollah et al., 2004). Although it is plausible to offer conjecture of specific removal mechanisms that occurred, further research is required to confirm the primary removal mechanisms based on experimental data for each estrogenic compound.

3.2. Kinetic study

3.2.1. Reaction kinetics

In this work, removal kinetics of E1, E2, E3, and EE2 were evaluated (Fig. 4 and Table 1) for experiments at constant volume, current density, conductivity, stir rate, and polarity reversal that achieved the greatest estrogen removal determined previously (16.7 mA cm^{-2}, 1000 mS cm^{-1}, 500 rpm, and 30 s polarity reversal). The reaction kinetics for the pseudo first-order relationship are plotted in Fig. 4 and listed in Table 1. Table 1 also contains the data for the second-order rate model and the Lagergren's first- and second- order relationship kinetic rate constants, including calculated q_e, and R^2.

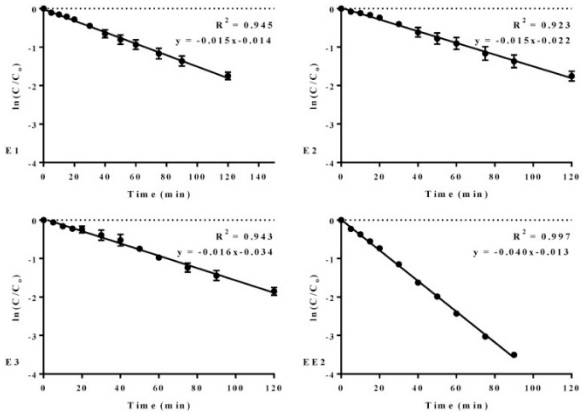

Fig. 4. Reaction kinetics for the pseudo first-order relationship between ln (C/Co) and electrocoagulation time. The error bars represent the standard error of the mean between triplicate tests.

Table 1. Pseudo first- and second-order kinetic removal rate constants, pseudo first- and second-order Lagergren adsorption kinetic removal rate constants, coefficient of determination (R^2), sum of least squares, and calculated q_e for various estrogenic compounds using iron electrocoagulation.

Estrogen	Pseudo first-order			Second-order		
	k' (min−1)	R2	SLS	k2 (µg min−1 L−1)	R2	SLS
E1	0.015	0.95	128	0.00018	0.91	6162
E2	0.015	0.92	436	0.00016	0.88	13100
E3	0.016	0.94	522	0.0002	0.73	19670
EE2	0.040	1.00	157	0.0014	0.83	39342

Estrogen	Lagergren's First-order				Lagergren's Second-order			
	k1 (min−1)	Calculated qe (µg g−1)	R2	SLS	k2 (g µg−1 min−1)	Calculated qe (µg g−1)	R2	SLS
E1	0.025	44.5	0.99	3195	0.00024	58	0.77	1462
E2	0.025	53.6	0.98	9471	0.00012	80	0.59	2949
E3	0.024	53.6	0.97	8481	0.00014	74	0.66	2612
EE2	0.040	56.3	0.99	240	0.00062	65	0.96	1549

*SLS: Sum of Least Squares.

The least-square method was used to determine the kinetic parameters for the model equation with the best fit. The R^2 and the sum of squared residuals were compared for each relationship. The estrogen EC degradation data fit best to the pseudo first-order model (Table 1). The second-order and Lagergren's first- and second- order kinetic relationship fit well in terms of R^2 values (see Table 1), however, the sum of squared residuals for all compounds were larger than that for the pseudo first-order model. Thus, the data demonstrated stronger pseudo-first order behavior ($R^2 > 0.99$), consistent with electrochemical oxidation studies for E1, E2, E3, and EE2 (Murugananthan et al., 2007; Feng et al., 2010b; Chen and Huang, 2013; Brocenschi et al., 2016). This may imply the mechanism of removal is predominantly oxidation as opposed to adsorption.

The pseudo-first order kinetic rates for E1, E2, and E3 were significantly less than the kinetic rate for EE2 (ANOVA p-value <0.0001; Tukey p-values for E1, E2 and E3 compared to EE2 were all <0.0001). EE2 was removed more than the natural estrogens (E1, E2, and E3) regardless of the parameters. This could be due to the higher k_{ow} and thus a greater adsorption capability than E1, E2, or E3. Additionally, there

may be a greater possibility for oxidation of EE2 due to the variation of the functional group attached to the C17 position on the cyclopentane ring (Hauser-Davis and Parente, 2018).

3.3. Energy use and estrogen degradation

Energy use is partially dependent upon the current density and conductivity. A high current density with a low conductivity increases the energy expended (Section S6 in SI, Fig. S2). The lowest energy use occurred at 4.16 mA cm^{-2} and a conductivity of 1000 µS cm^{-1} while the highest was with a current density of 16.7 mA cm^{-2} and a conductivity of 500 µS cm^{-1}. This was expected because with low current and a high conductivity there will be a smaller IR-drop (Mollah et al., 2004). However, a current density of 4.16 mA cm^{-2} was not capable of providing enough potential to remove estrogens (Fig. 5). A current density of 16.7 mA cm^{-2} and a conductivity of 1000 µS cm^{-1} provided estrogen removal with minimal energy use and less electrolyte addition. The three systems with largest estrogen removal normalized to energy use (µmoles kWh^{-1}) were not significantly different (500, 1000, or 3000 µS cm^{-1} at 16.7 mA cm^{-2}) for any compound (Tukey p-values ≥ 0.2), with the exception of significantly less EE2 removal at 3000 µS cm^{-1} compared to 500 µS cm^{-1} at 16.7 mA cm^{-2} (Tukey p-value = 0.003).

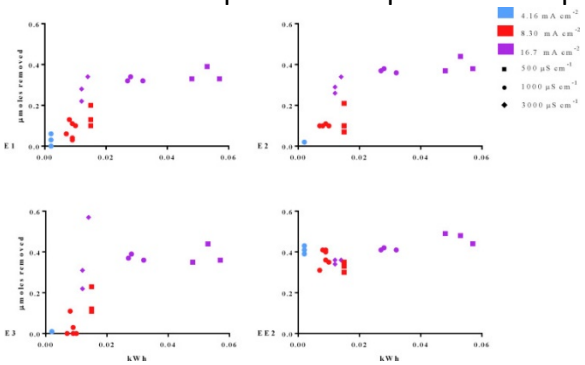

Fig. 5. Comparison of µmoles of E1, E2, E3, and EE2 removed per kWh used. Conductivity (µS cm−1) is grouped by shape and current density (mA cm−2) is grouped by color. (For interpretation of the references to color in this figure legend, the reader is referred to the Web version of this article.)

3.4. Floc characterization

During the EC process, the iron floc formed within the reactor, turning the clear solution to a turbid orange-brown color. To characterize the reactor in general, floc characterization was completed to understand the structure, charge, size, shape and main components of reactor performance. The information collected here provides information on the nature of the flocs formed and the potential to remove estrogenic compounds.

3.4.1. X-ray diffraction

XRD analysis was conducted on iron floc samples that were collected and freeze-dried to determine their crystalline phases. Strong peaks at 2ϑ of 13.9°, 27.0°, 36.3°, and 46.8° were observed from the XRD patterns, suggesting the formation of lepidocrocite (γ-FeOOH) as the dominant product (see SI section S7, Fig. S3). Lepidocrocite has been reported as a typical oxidation product of Fe^{2+} by dissolved oxygen under ambient conditions (Cornell et al., 2003), and results are consistent with previous studies that applied EC for inorganic pollutant removal with iron electrodes (Wan et al., 2011).

3.4.2. Zeta potential

Zeta potential measurements of the iron floc (γ-FeOOH) indicate a point of zero charge (PZC) of 5.67 and an average floc diameter of 2255 nm. For comparison, data from literature reports PZCs values for

γ-FeOOH of 6.7–7.45 and the dissociation constants are approximately 6.3 and 8.3 (Cornell et al., 2003). From these measured values and literature values, when the charge of the floc is net positive, no deprotonated estrogenic compounds are present as E1, E2, E3, and EE2 have acid-dissociation constants greater than 10.3 (see Table S9 in SI), however, many experiments had final pH values of 10 and greater and still had little removal. The bulk solution pH influences the surface charge of the iron hydroxide flocs, and thus the PZC. When the pH of the solution is greater than the PZC, the net surface charge of the floc carries a net negative charge and will repulse anions (Tong et al., 2016). Thus, adsorption of estrogens to iron oxide floc due to direct coulombic attraction is unlikely.

Additionally, assuming the electrode has a similar PZC, when the zeta potential is zero around the point of zero charge, the ionic electrical double layer (EDL) is absent, decreasing the overall distance to the electrode, thereby improving the possibility for direct electrode redox reactions (Bagotsky, 2005). Another important factor is that in highly concentrated ionic solutions, the potential is very small and the diffuse EDL collapses against the electrode surface, which also decreases the distance to the electrode surface for direct redox reactions (Bagotsky, 2005).

3.4.3. SEM and EDX analyses

The SEM photographs of the iron floc at magnifications of×55, ×500, and ×650 are in Section S8, Fig. S4 in the SI. The photos indicate that at ×55 and ×500, the micrometer-sized particles are crystalline and are plate like in overall structure. This is consistent with lepidocrocite, which is commonly formed via Fe^{2+} systems (Cornell et al., 2003). The EDX analysis (see section S8, Fig. S5 in SI) suggested that the major components of the floc are iron and oxygen.

4. Conclusions

The purpose of this research was to determine the potential for estrogen removal, the parameters to achieve that removal, the kinetics of removal, and the characteristics of the floc formed within the reactor. The results from this study provide knowledge on the use of EC for the removal of uncharged organic micropollutants and give an indication of mechanism via the kinetic relationship best followed by the removal. The EC process was successfully applied to remove estrogenic compounds from water. The operation parameters to achieve the greatest removal specifically in this study were 16.7 mA cm^{-2}, 1000 μS cm^{-1}, 30 s polarity reversal time, and a stir rate of 500 rpm. Average removal efficiencies for E1, E2, E3, and EE2 were 81%, 87%, 85%, and 97%, respectively. With increasing conductivity, there was no significant increase in removal, but there was a decrease in potential required. An increase in current density, because of increasing current, correlated well with an increase in overall estrogenic compound removal. An investigation into polarity reversal determined that shorter polarity reversal time using an iron EC two electrode reactor increased removals of estrogenic compounds, likely due to decreased passivation at the electrode surface. A number of kinetic models were applied and compared for E1, E2, E3, and EE2 and all compound removal followed pseudo-first order kinetics. Characterization of the floc produced during EC showed that the charge at neutral pH was negative. XRD analyses determined the major species present was lepidocrocite. These findings suggest that EC using iron electrodes has great potential for use in water treatment, as it is capable of removing estrogenic compounds in water. More research is required to understand the removal mechanisms, electrode material passivation, and impact of water characteristics.

Acknowledgements

This research was supported by the National Science Foundation (NSF) under Grant No. 1433003. All opinions expressed in the paper are the authors' and do not necessarily reflect the views of NSF. The authors acknowledge the use of the LC-MS from Marquette University, funded by the GHR Foundation. The authors acknowledge the use of the XRD instrument in the Advanced Analysis Facility at the University of Wisconsin-Milwaukee. We are grateful to A/O Smith Corporation, Brookfield, WI, for providing electrodes and polarity switchbox. Funding for K O'Malley was provided by the Industry University Collaborative Research Program for Water Equipment & Policy in Milwaukee, Wisconsin, USA, under National Science Foundation, USA Grant number 0968844.

References

Al-Shannag et al., 2015 M. Al-Shannag, Z. Al-Qodah, K. Bani-Melhem, M.R. Qtaishat, M. Alkasrawi **Heavy metal ions removal from metal plating wastewater using electrocoagulation: kinetic study and process performance** Chem. Eng. J., 260 (2015), pp. 749-756

Bagotsky, 2005 V.S. Bagotsky **Fundamentals of Electrochemistry** John Wiley & Sons (2005)

Benotti et al., 2009a M.J. Benotti, R.a. Trenholm, B.J. Vanderford, J.C. Holady, B.D. Stanford, S.a. Snyder **Pharmaceuticals and endocrine disrupting compounds in U.S. drinking water** Environ. Sci. Technol., 43 (2009), pp. 597-603

Benotti et al., 2009b M.J. Benotti, R.A. Trenholm, B.J. Vanderford, J.C. Holady, B.D. Stanford, S.A. Snyder **Pharmaceuticals and endocrine disrupting compounds in U.S. drinking water** Environ. Sci. Technol., 43 (2009), pp. 597-603

Brocenschi et al., 2016 R.F. Brocenschi, R.C. Rocha-Filho, N. Bocchi, S.R. Biaggio **Electrochemical degradation of estrone using a boron-doped diamond anode in a filter-press reactor** Electrochim. Acta, 197 (2016), pp. 186-193

Caldwell et al., 2010 D.J. Caldwell, F. Mastrocco, E. Nowak, J. Johnston, H. Yekel, D. Pfeiffer, M. Hoyt, B.M. DuPlessie, P.D. Anderson **An assessment of potential exposure and risk from estrogens in drinking water** Environ. Health Perspect., 118 (2010), pp. 338-344

Chen and Huang, 2013 T.S. Chen, K.L. Huang **Effect of operating parameters on electrochemical degradation of estriol (E3)** International journal of electrochemical science, 8 (2013), pp. 6343-6353

Chen et al., 2000 X. Chen, G. Chen, P.L. Yue **Separation of pollutants from restaurant wastewater by electrocoagulation** Separ. Purif. Technol., 19 (2000), pp. 65-76

Cong et al., 2014 V.H. Cong, S. Iwaya, Y. Sakakibara **Removal of estrogens by electrochemical oxidation process** J. Environ. Sci., 26 (2014), pp. 1355-1360

Conley et al., 2017 J.M. Conley, N. Evans, H. Mash, L. Rosenblum, K. Schenck, S. Glassmeyer, E.T. Furlong, D.W. Kol pin, V.S. Wilson **Comparison of in vitro estrogenic activity and estrogen concentrations in source and treated waters from 25 U.S. drinking water treatment plants** Sci. Total Environ., 579 (2017), pp. 1610-1617

Cornell et al., 2003 R.M. Cornell, U. Schwertmann, John Wiley & Sons **The Iron Oxides : Structure, Properties, Reactions, Occurrences, and Uses** Wiley-VCH (2003)

Crittenden et al., 2012a J.C. Crittenden, C. John, R.R. Trussell, D.W. Hand, K.J. Howe, G. Tchobanoglous **MWH's Water Treatment : Principles and Design** John Wiley & Sons, Hoboken (2012)

Crittenden et al., 2012b J.C. Crittenden, R.R. Trussell, D.W. Hand, K.J. Howe, G. Tchobanoglous **MWH's Water Treatment: Principles and Design** (third ed.), Wiley (2012)

Daughton and Ternes, 1999 C.G. Daughton, T.A. Ternes **Pharmaceuticals and personal care products in the environment: agents of subtle change?** Environ. Health Perspect., 107 (Suppl. l) (1999), pp. 907-938

Dubrawski and Mohseni, 2013 K.L. Dubrawski, M. Mohseni **Standardizing electrocoagulation reactor design: iron electrodes for NOM removal** Chemosphere, 91 (2013), pp. 55-60

Feng et al., 2010a Y. Feng, C. Wang, J. Liu, Z. Zhang **Electrochemical degradation of 17-alpha-ethinylestradiol (EE2) and estrogenic activity changes** J. Environ. Monit., 12 (2010), pp. 404-408

Feng et al., 2010b Y. Feng, C. Wang, J. Liu, Z. Zhang, Y. Feng, C. Wang, J. Liu, Z. Zhang, G. Yu, M. Crane, C.R. Tyler, M.J. Waldock, J.P. Sumpter, C.R. Tyler **Electrochemical degradation of 17-alpha-ethinylestradiol (EE2) and estrogenic activity changes** J. Environ. Monit., 12 (2010), pp. 404-408

Ghatak, 2014 H.R. Ghatak **Comparative removal of commercial diclofenac sodium by electro-oxidation on platinum anode and combined electro-oxidation and electrocoagulation on stainless steel anode** Environ. Technol., 35 (2014), pp. 2483-2492

Hauser-Davis and Parente, 2018 R.A. Hauser-Davis, T.E. Parente **Ecotoxycology: Perspectives on Key Issues** (2018)

Heffron et al., 2016 J. Heffron, M. Marhefke, B.K. Mayer **Removal of trace metal contaminants from potable water by electrocoagulation** Sci. Rep. (2016), pp. 1-9

Heidmann and Calmano, 2008 I. Heidmann, W. Calmano **Removal of Cr(VI) from model wastewaters by electrocoagulation with Fe electrodes** Separ. Purif. Technol., 61 (2008), pp. 15-21

Holt et al., 2005 P.K. Holt, G.W. Barton, C.a. Mitchell **The future for electrocoagulation as a localised water treatment technology** Chemosphere, 59 (2005), pp. 355-367

Keenan and Sedlak, 2008 C.R. Keenan, D.L. Sedlak **Ligand-enhanced reactive oxidant generation by nanoparticulate zero-valent iron and oxygen** Environ. Sci. Technol., 42 (2008), pp. 6936-6941

Khatibikamal et al., 2010 V. Khatibikamal, A. Torabian, F. Janpoor, G. Hoshyaripour **Fluoride removal from industrial wastewater using electrocoagulation and its adsorption kinetics** J. Hazard Mater., 179 (2010), pp. 276-280

Kidd et al., 2007 K.A. Kidd, P.J. Blanchfield, K.H. Mills, V.P. Palace, R.E. Evans, J.M. Lazorchak, R.W. Flick **Collapse of a fish population after exposure to a synthetic estrogen** Proc. Natl. Acad. Sci. Unit. States Am., 104 (2007), pp. 8897-8901

Kolpin et al., 2002 D.W. Kolpin, E.T. Furlong, M.T. Meyer, E.M. Thurman, S.D. Zaugg, L.B. Barber, H.T. Buxton **Pharmaceuticals, hormones, and other organic wastewater contaminants in U.S. streams, 1999-2000: a national reconnaissance** Environ. Sci. Technol., 36 (2002), pp. 1202-1211

Kuch and Ballschmiter, 2001 H.M. Kuch, K. Ballschmiter **Determination of endocrine-disrupting phenolic compounds and estrogens in surface and drinking water by HRGC-(NCI)-MS in the picogram per liter range** Environ. Sci. Technol., 35 (2001), pp. 3201-3206

Lai et al., 2000 K.M. Lai, K.L. Johnson, M.D. Scrimshaw, J.N. Lester **Binding of waterborne steroid estrogens to solid phases in river and estuarine systems** Environ. Sci. Technol., 34 (2000), pp. 3890-3894

Li et al., 2012 L. Li, C.M. Van Genuchten, S.E.A. Addy, J. Yao, N. Gao, A.J. Gadgil **Modeling As(III) oxidation and removal with iron electrocoagulation in groundwater** Environ. Sci. Technol., 46 (2012), pp. 12038-12045

Lin et al., 2015 H. Lin, Y. Wang, J. Niu, Z. Yue, Q. Huang **Efficient sorption and removal of perfluoroalkyl acids (PFAAs) from aqueous solution by metal hydroxides generated in situ by electrocoagulation** Environ. Sci. Technol., 49 (2015), pp. 10562-10569

Liu et al., 2010 H. Liu, X. Zhao, J. Qu **Electrocoagulation in water treatment** C. Comninellis, G. Chen (Eds.), Electrochemistry for the Environment, Springer New York, New York, NY (2010), pp. 245-262

Liu et al., 2009 Z.-H. hua Liu, Y. Kanjo, S. Mizutani **Removal mechanisms for endocrine disrupting compounds (EDCs) in wastewater treatment - physical means, biodegradation, and chemical advanced oxidation: a review** Sci. Total Environ., 407 (2009), pp. 731-748

Martins et al., 2011 A.F. Martins, C.A. Mallmann, D.R. Arsand, F.M. Mayer, C.G.B. Brenner **Occurrence of the antimicrobials sulfamethoxazole and trimethoprim in hospital effluent and study of their degradation products after electrocoagulation** Clean. - Soil, Air, Water, 39 (2011), pp. 21-27

Mission et al., 2010 E.G. Mission, P.D. Gaspillo, L.P. Belo, G.T. Cruz **Treatment of ibuprofen in simulated wastewater through compact electrocoagulation process** Proceedings of the 5th Erdt Conference (2010), pp. 2094-2516

Mohora et al., 2012 E. Mohora, S. Rončević, B. Dalmacija, J. Agbaba, M. Watson, E. Karlović, M. Dalmacija **Removal of natural organic matter and arsenic from water by electrocoagulation/flotation continuous flow reactor** J. Hazard Mater., 235 (2012), pp. 257-264

Mollah et al., 2004 M. Mollah, P. Morkovsky, J. Gomes, M. Kesmez, J. Parga, D. Cocke **Fundamentals, present and future perspectives of electrocoagulation** J. Hazard Mater., 114 (2004), pp. 199-210

Moussout et al., 2018 H. Moussout, H. Ahlafi, M. Aazza, H. Maghat **Critical of linear and nonlinear equations of pseudo-first order and pseudo-second order kinetic models** Karbala international journal of modern science, 4 (2018), pp. 244-254

Murugananthan et al., 2007 M. Murugananthan, S. Yoshihara, T. Rakuma, N. Uehara, T. Shirakashi **Electrochemical degradation of 17β-estradiol (E2) at boron-doped diamond (Si/BDD) thin film electrode** Electrochim. Acta, 52 (2007), pp. 3242-3249

National Institute of Environmental Health Sciences, 2010 National Institute of Environmental Health Sciences **Endocrine Disruptors** (2010)

Pan et al., 2016 C. Pan, L.D. Troyer, J.G. Catalano, D.E. Giammar **Dynamics of chromium(VI) removal from drinking water by iron electrocoagulation** Environ. Sci. Technol., 50 (2016), pp. 13502-13510

Rajeshwar et al., 1994 K. Rajeshwar, J.G. Ibanez, G.M. Swain **Electrochemistry and the environment** J. Appl. Electrochem., 24 (1994), pp. 1077-1091

Roy et al., 2009 J.R. Roy, S. Chakraborty, T.R. Chakraborty **Estrogen-like endocrine disrupting chemicals affecting puberty in humans--a review** Med. Sci. Mon. Int. Med. J. Exp. Clin. Res.: international medical journal of experimental and clinical research, 15 (2009), pp. RA137-R145

Silva et al., 2012 C.P. Silva, M. Otero, V. Esteves **Processes for the elimination of estrogenic steroid hormones from water: a review** Environmental Pollution, Elsevier (2012), pp. 38-58

Snyder et al., 2004 S. Snyder, E. Wert, D. Rexing, Southern Nevada Water Authority, P. Westerhoff, Y. Yoon **Conventional and advanced water treatment processes for**

the removal of endocrine disruptors and pharmaceuticals Water Quality Conference (2004), pp. 247-264

Snyder et al., 2006 S.A. Snyder, E.C. Wert, D.J. Rexing, R.E. Zegers, D.D. Drury **Ozone oxidation of endocrine disruptors and pharmaceuticals in surface water and wastewater** Ozone: Sci. Eng., 28 (2006), pp. 445-460

Snyder et al., 2003 S.A. Snyder, P. Westerhoff, Y. Yoon, D.L. Sedlak **Pharmaceuticals, personal care products, and endocrine disruptors in water: implications for the water Industry** Environ. Eng. Sci., 20 (2003)

Ternes, 1998 T.A. Ternes **Occurrence of drugs in German sewage treatment plants and rivers** Water Res., 32 (1998), pp. 3245-3260

Timmes et al., 2010 T.C. Timmes, H.C. Kim, B.A. Dempsey **Electrocoagulation pretreatment of seawater prior to ultrafiltration: pilot-scale applications for military water purification systems** Desalination, 250 (2010), pp. 6-13

Tong et al., 2016 Y. Tong, B.K. Mayer, P.J. McNamara **Triclosan adsorption using wastewater biosolids-derived biochar** Environmental science: water research & technology, 2 (2016), pp. 761-768

US EPA, 2016 US EPA Contaminant Candidate List 4 - CCL, 4 4 (2016), p. 2

Vajda et al., 2008 A.M. Vajda, L.B. Barber, J.L. Gray, E.M. Lopez, J.D. Woodling, D.O. Norris **Reproductive disruption in fish downstream from an estrogenic wastewater effluent** Environ. Sci. Technol., 42 (2008), pp. 3407-3414

Wan et al., 2011 W. Wan, T.J. Pepping, T. Banerji, S. Chaudhari, D.E. Giammar **Effects of water chemistry on arsenic removal from drinking water by electrocoagulation** Water Res., 45 (2011), pp. 384-392

Westerhoff et al., 2005 P. Westerhoff, Y. Yoon, S. Snyder, E. Wert **Fate of endocrine-disruptor, pharmaceutical, and personal care product chemicals during simulated drinking water treatment processes** Environ. Sci. Technol., 39 (2005), pp. 6649-6663

Yoshihara and Murugananthan, 2009 S. Yoshihara, M. Murugananthan **Decomposition of various endocrine-disrupting chemicals at boron-doped diamond electrode** Electrochim. Acta, 54 (2009), pp. 2031-2038

Appendix A. Supplementary data

The following is the Supplementary data to this article:

Download Word document (15MB)

Help with docx files

Multimedia component 1.

Table of Contents

S1: Physical-chemical properties of estrogenic compounds

Table S1. Physical-chemical properties of estrogenic compounds

Property	Estrone (E1)	17β-Estradiol (E2)	Estriol (E3)	17α-Ethynylestradiol (EE2)
Molecular Formula	$C_{18}H_{22}O_2$	$C_{18}H_{24}O_2$	$C_{18}H_{24}O_3$	$C_{20}H_{24}O_2$
CAS No.	53-16-7	50-28-2	50-27-1	57-63-6
Source	Natural	Natural	Natural	Synthetic
Molecular Weight (g/mol)[56]	270.4	272.4	288.4	296.403
Log K_{OW} [56]	3.43	3.94	2.81	4.15
pKa [57]	10.5-10.7	10.3-10.8	10.3-10.8	10.4 [58]

S2: Liquid Chromatography-Mass Spectrometry Methods

Table S2. LC-MS Parameters

Parameter	Value
Eluent Type:	Gradient
Mobile Phase A:	Milli-Q water
Mobile Phase B:	Methanol
Flow Rate:	0.4 mL/min
Column Temperature:	35°C
Detection:	Electrospray Mass Spec (ESMS) at 40°C
Injection Volume:	15 µL
Acquisition Mode:	SIM
Interface Temperature:	350°C
DL Temperature:	250°C
Nebulizer Gas Flow:	1.5 L/min
Heat Block:	400°C

Drying Gas Flow:	15 L/min

Table S3. Liquid Chromatography Gradient Flow

Gradient:	Time (min)	Mobile Phase A	Mobile Phase B
Profile:	0	65	35
	0.6	35	65
	7.5	35	65
	8.5	15	85
	13	15	85
	13.01	35	65
	15	65	35
	16	STOP	STOP

S3: Standard Curve, Limit of Detection (LOD), and Limit of Quantification (LOQ) Criteria

Standard Curve: Ten standards at concentrations of approximately 1.56, 3.13, 6.25, 12.5, 25, 50, 100, 200, 400, and 800 µg L^{-1} were prepared for each test in the same manner as the synthetic surface water solution to emulate the impact of water quality parameters on the potential ion suppression during LC-MS analysis. The number of standards used to analyze the data was dependent upon the limit of detection (LOD) and limit of quantification (LOQ) for that specific surface water solution, as described in section 2.6.1. The number of standards for each test ranged from 6 to 10 depending upon the compound (E1, E2, E3, or EE2). The appropriate R^2 range according to a Table of Critical Values from the Pearson Correlation with degrees of freedom from 4 to 6 at 99.5 percent confidence would be 0.99 and 0.917[59].

LOD and LOQ: The LOD and LOQ were based on the signal-to-noise ratio (S/N) reported from the LC-MS software from Shimadzu for each standard curve prepared. The LOD was defined as having an S/N of 1:3 or greater and the LOQ was defined as having an S/N of 1:10 or greater. Non-detect samples were set to the LOD, while samples with peaks of S/N less than 10 were set to the LOQ.

S4: Test Data

Table S4. Experimental operation parameters and final pH

Current Density (mA cm-2)	Polarity Reversal Time (s)	Conductivity µS cm-1	Stir Rate (rpm)	pH	Final pH
4.16	30	962	500	6.94	10.51
4.16	30	962	500	6.94	10.17
4.16	30	962	500	6.94	10.54
16.7	30	1017	50	7.09	9.4
16.7	30	1017	50	7.09	9.04
16.7	30	1017	50	7.09	9.8
16.7	30	975	50	7.08	9.88
16.7	30	1000	120	7.06	7.35
16.7	30	1000	120	7.06	8.31
16.7	30	1000	120	7.06	6.94

16.7	30	512	500	7.04	8.15
16.7	30	512	500	7.04	8.43
16.7	30	512	500	7.04	7.64
16.7	30	1000	500	6.98	7.46
16.7	30	1000	500	6.98	7.84
16.7	30	1000	500	6.98	7.68
16.7	30	3000	500	6.97	8.38
16.7	30	3000	500	6.99	6.71
16.7	30	3000	500	6.99	7.03
8.3	30	1000	500	7.04	8.69
8.3	30	1000	500	7.04	10.33
8.3	30	1000	500	7.04	10.39
16.7	30	1002	500	7.05	7.83
16.7	30	1002	500	7.05	9.71
16.7	30	1002	500	7.05	9.86
16.7	30	1016	500	7.06	7.89
16.7	30	1016	500	7.06	7.68
16.7	30	1016	500	7.06	7.95
16.7	120	988	500	7.06	8.73
16.7	120	988	500	7.06	8.51
16.7	120	988	500	7.06	8.62
16.7	240	923	500	7.06	10.17
16.7	240	923	500	7.06	9.53
16.7	240	923	500	7.06	9.33

S5: Conductivity

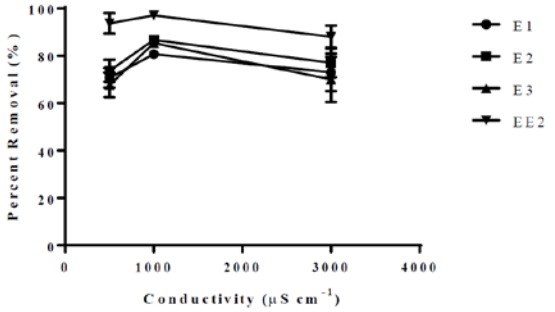

Fig. S1. Conductivity impacted removal for E1, E2, and E3 only between 500 and 1000 µS cm^{-1} (*p*-values ≤ 0.0007) and 500 and 3000 µS cm^{-1} (*p*-values ≤ 0.002). There was no significant difference in E1, E2, and E3 removal between conductivities of 1000 and 3000 µS cm^{-1} (*p*-values ≥ 0.22) while maintaining a current density of 16.7 mA cm^{-2}. The time was 120 min of iron electrocoagulation at pH 7 with an initial estrogen concentration of approximately 200 µg L^{-1}. The error bars represent the standard error of the mean.

S6: Energy Use and Degradation

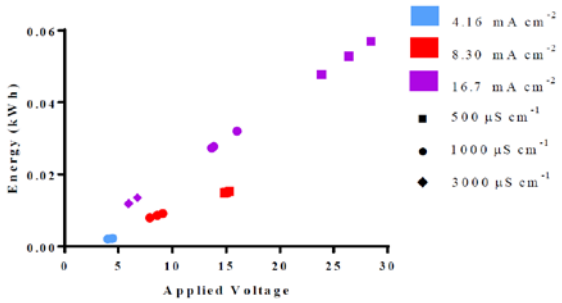

Fig. S2. Energy versus applied voltage for the various EC systems investigated. Conductivity (µS cm^{-1}) is grouped by shape and current density (mA cm^{-2}) is grouped by color.

S7: X-Ray Diffraction Patterns

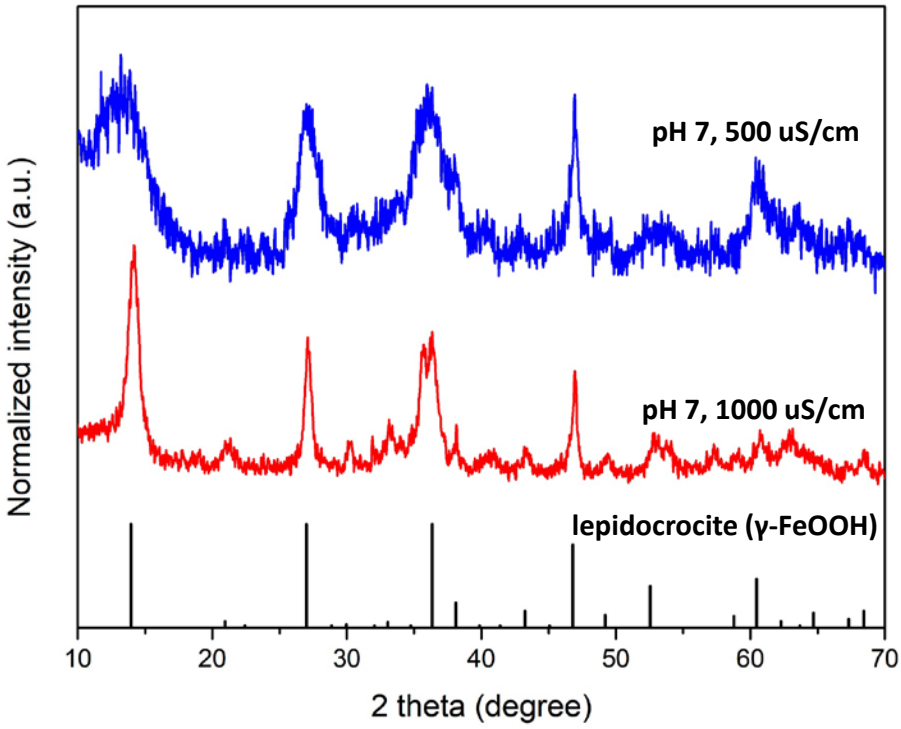

Fig. S3. XRD patterns of iron flocs produced during electrocoagulation. The reference pattern for lepidocrocite (01-0136) is included for comparison.

S8: SEM and EDX Results

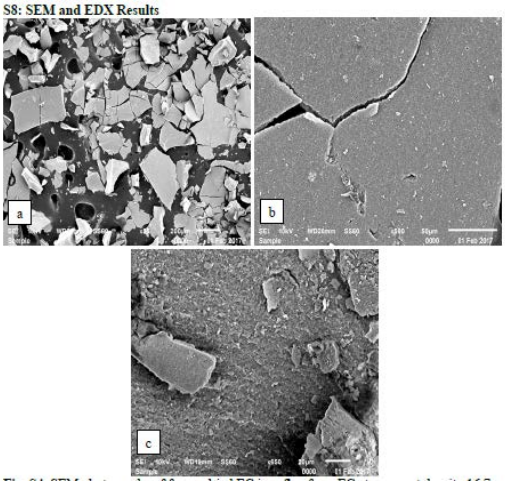

Fig. S4. SEM photographs of freeze dried EC iron floc from EC at a current density 16.7 mA cm^{-2} for 120 minutes, pH 7, and conductivity of 1000 µS cm^{-1} at magnifications of x55 (a), x500 (b), and x650 (c).

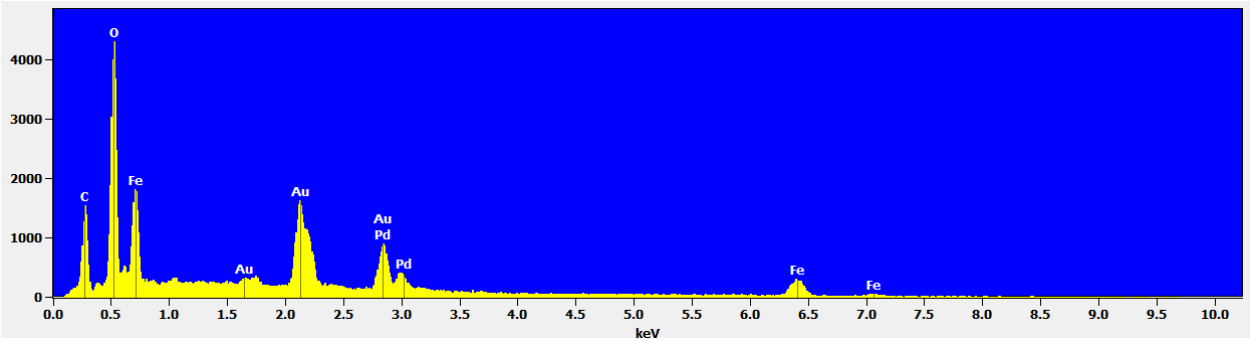

Fig. S5. EDX data showing the main components of the iron oxide floc consist mainly of iron and oxygen.